ERF2011_109

AERO-ELASTIC MODELING OF HELICOPTER COMPOSITE BLADE IN UNSTEADY INCOMPRESSIBLE FLOW

T. Farsadi [#]
Department of Aerospace Engineering
Sharif Tech. University
Tehran, IRAN
Phone: (+90)-(537)- 5213780
E-mail: touraj.farsadi@gmail.com

J. Javanshir [#]
Department of Aerospace Engineering
Middle East Tech. University
Ankara, TURKEY
Phone: (+90)-(312)-2102433
E-mail: jaberjavanshir@hotmail.com

ABSTRACT

In this study, the composite helicopter rotor blade is modeled as an "*Elastic Cantilevered Rotating Thin-Walled Composite Box Beam* " with angular velocity (Ω) and forward flight speed (U_n). The present "*Circumferentially Asymmetric Stiffness (CAS)*" structural model takes into account a group of non-classical effects; such as the transverse shear, the material anisotropy, warping inhibition, etc. The "*Aerodynamic Strip Method*" based on "*Wagner Function*" in unsteady incompressible flow are used to simulate incompressible unsteady aerodynamic effects. As a result, the "*Extended Galerkin's Method (EGM)*" and the "*Separation of Variables Method*" are used to obtain the coupled and linear "*Governing System of Dynamic Equations*". Solving the aforementioned equations of motion in the time domain, the aeroelastic responses of the "*Composite Rotor Blade*" can be computed. The present numerical results were compared and are verified with existing results in the literature. Based on these, some important conclusions are presented.

INTRODUCTION AND BRIEF REVIEW

The aeroelastic analysis to predict the characteristics of rotorcraft systems is very important in the aerodynamic and structural design of composite helicopter blades. More recently, the "Advanced Composites" are increasingly being used in rotorcraft blades and structures due to their favorable characteristics [1]. Nowadays, more than %40 of the latest rotorcraft structures is made of various types of "Advanced Composites". The so-called "Advanced Composites" generally exhibit certain advantageous properties such as high strength, effective stiffness, light-deadweight, high resistance to sonic and other dynamic fatigue – fracture, reduced vibrational response, increased aerodynamic and structural stability and flight safety. The fiber orientations in the material layers of these composites can be used to provide the desired elastic lay-up with the right material and stiffness properties.

The investigation of the aeroelastic stability is extremely important from the design and operational point of view of rotor blades. The aeroelastic response problem which represents the blade free and forced (under aerodynamic and other loads) vibration responses is critical in the safety and air – worthiness of flight vehicle systems.

Most of the structural dynamic models for the rotor blades are moderate deflection-type beam theories that are based on ordering schemes and are valid for moderate deflections. These models have frequently been applied to the aeroelastic stability and response analysis for isotropic [2-4] and composite hingeless rotor blades [5,6].

Numerous researches have been conducted on rotating composite thin-walled beams. Rehfield [7] studied the design analysis methodology of a thin-walled beam for composite rotor blades. Rehfield et al. [8] discussed the non-classical behavior of thin-walled composite beams with closed cross sections. Chandra and Chopra [9] investigated the vibration characteristics of rotating composite box beams by experiment and theoretical methods. Smith and Chopra [10] researched the aeroelastic response, loads and stability of a composite thin walled beam. In the case of the rotating beam, Song et al. [11] researched the vibration of rotating blades modeled as anisotropic thin-walled beams containing piezoelectric materials through the proportional control law and velocity control law. In the past few years, a number of analytical models of anisotropic "Thin-Walled Composite Box Beams" have been proposed in the world-wide literature and they are analyzed either numerically or experimentally. One of them, a refined "Thin-Walled Composite Box Beam" theory developed by Librescu and Song [12] and Song [13] has been extensively used for the study of the free vibrations, Furthermore, Qin and Librescu [14] and Qin [15] have investigated the "dynamic aeroelastic response of aircraft wings" modeled as anisotropic "Thin-Walled Composite Box Beams" exposed to gust and blast loads**.** Haddadpour and Shadmehri [16] have investigated the effect of the offset between the reference axis and the mid-chord on aeroelastic stability of composite wings in an incompressible flow.

[#] Graduate student

THEORETICAL ANALYSIS AND FORMULATION

"Rotating Thin-Walled Composite Box Beam" as "Structural Model"

The analysis of rotating blade structures is more complex than that of their nonrotating counterparts. In the rotating case, in addition to the accelerations resulting from elastic structural deformations, the centrifugal and coriolis accelerations have to be included in the modeling.

Here in this present study, the structural model is similar to those developed in Ref. [16, 17].

Inertial reference coordinate (X,Y,Z) is attached to the hub centre, while two other coordinate systems exist (x,y,z) as a local coordinate associated with the blade and (n,s,z) used to define complex cross-section profiles (Figure. (1), (2) and (3)).

Let (x,y,z) be a fixed Cartesian coordinate system with the outward *z*-direction parallel to the longitudinal axis of the "Rotating Thin-Walled Composite Box Beam" as shown in Figures.(1) and (2). The thickness, along its contour of the "Composite Box Beam", is assumed to be constant "h" as given in the same Figures.(1) and (2).

The angular velocity is also assumed to be constant and is directed in the $(X-Z)$-plane (Figure. (3)). The position vector "R" of a point in a deformed rotating beam, measured from the centre of the hub, can be expressed as [17],

$$\begin{cases} P = P_0 + P_v + \Delta \\ R_0 = R_0 k, \quad R_u = xi + yj + zk = ui + vj + wk \end{cases} \tag{1}$$

Considering angular velocity (Ω) and Eq. (1), "$\dot{R}$" and "$\ddot{R}$" can be written as,

$$\begin{cases} \dot{R} = \left[\dot{u} + \Omega(R_0 + z + w)\right] i + \dot{v} j + \left[\dot{w} - \Omega(x + u)\right] k \\ \ddot{R} = \left[\ddot{u} + 2\dot{w}\Omega - (x + u)\Omega^2\right] i + \ddot{v} j \\ \qquad + \left[\ddot{w} - 2\dot{u}\Omega - (R_0 + z + w)\Omega^2\right] k \end{cases} \tag{2}$$

"R_0" and "R_u" are the hub radius and the undeformed position vector of a beam point, respectively, and "Δ" represents the displacement vector, whose components are defined in Eq.(3).

A "Rotating Composite Thin-Walled Box Beam" with a length of "L", thickness of "h", and hub radius of "R_0" is considered in Figure. (2) and (3).

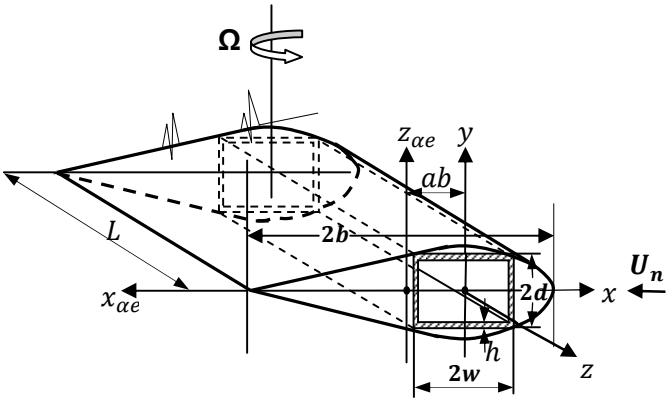

Figure. 1. Symbolic Rotor blade and "Thin-Walled Composite Box Beam" Configuration (Aerodynamic and Structural Coordinates)

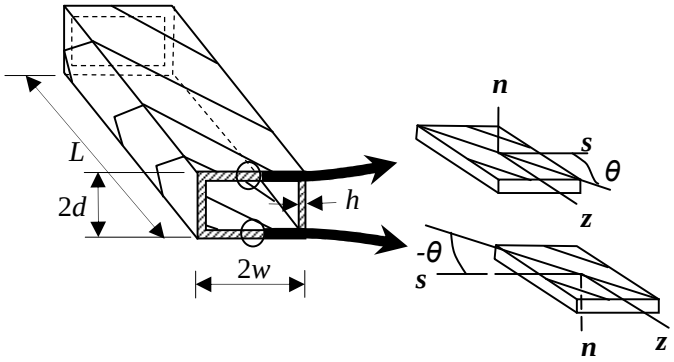

Figure. 2. "Thin-Walled Composite Box Beam" (Fiber Lay-up and "Circumferentially Asymmetric Stiffness (CAS)" Configuration) (Adopted from Librescu [17])

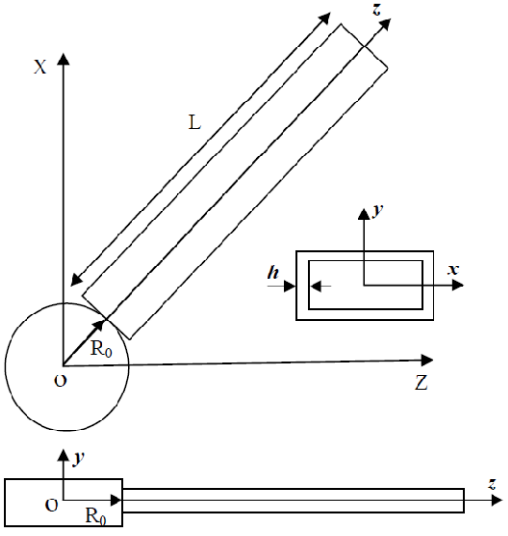

Figure. 3. Schematic description of the rotate blade structure simulated by "Rotating Thin-Walled Composite Beam" and its cross-section

In addition to the global (x, y, z) coordinate system, a local one (n, s, z) is introduced, where "*n*" and "*s*" are the normal and tangential directions to the contour, of the "Rotating Thin-Walled Composite Box Beam" respectively (see also Figures. (2)). The present structural model of the "Rotating Thin-Walled Composite Box Beam" includes some non-classical effects such as material anisotropy, transverse shear, primary and secondary warping inhibition, nonuniform torsional model and rotary moment of inertia [15-17]. Also, "Circumferentially Asymmetric Stiffness (CAS)" method [16, 17] is chosen among various lay-up methods in order to obtain an appropriate coupling for the rotor blade structural performance. This ply-angle configuration, achievable via the usual filament winding technology, results in an exact decoupling between the extension - twist, on one hand, and the flap – shear elastic coupling, on the other hand.

The 3-D displacement quantities $\left(u, v, w\right)$ are assumed to be,

$$\begin{cases} u(x,y,z,t) = u_0(z,t) - y\phi(z,t) \\ v(x,y,z,t) = v_0(z,t) + x\phi(z,t) \\ w(x,y,z,t) = w_0(z,t) + \theta_x(z,t)\left[y(s) - n\dfrac{dx}{ds}\right] + \theta_y(z,t)\left[x(s) + n\dfrac{dy}{ds}\right] \\ -\phi'(z,t)[F_w(s) + na(s)] \end{cases} \tag{3}$$

where,

$$\begin{cases} \theta_x(z,t) = \gamma_{yz}(z,t) - v_0'(z,t) \\ \theta_y(z,t) = \gamma_{xz}(z,t) - u_0'(z,t) \\ a(s) = -y(s)\dfrac{dy}{ds} - x(s)\dfrac{dx}{ds} \end{cases} \tag{4}$$

In the above Eqs.(3) and (4), $\left(u_0(z,t), v_0(z,t), w_0(z,t)\right)$ are the medium surface displacements in the "Rotating Thin-Walled Box Beam" in (x, y, z) directions, respectively. Similarly, $\left(\theta_x(z,t), \theta_y(z,t), \phi(z,t)\right)$ are the three rotations in (x, y, z) directions, respectively. Additionally, $\left(\gamma_{zy}(z,t), \gamma_{xz}(z,t)\right)$ represent the transverse shear strains. The other quantities in Eqs.(3) and (4) are as follows:

The primary "Warping Function (F_w)" is expressed as,

$$F_w = \int_0^s [r_n(s) - \Psi]ds \tag{5}$$

where the "Torsional Function (Ψ)" and the quantity " $r_n(s)$ " are given as,

$$\begin{cases} \Psi = \dfrac{\oint_C \dfrac{r_n(s)}{h(s)}ds}{\oint_C \dfrac{ds}{h(s)}} \\ r_n(s) = x(s)\dfrac{dy}{ds} - y(s)\dfrac{dx}{ds} \end{cases} \tag{6}$$

The strains contributing to the potential energy and kinematic energy are,

spanwise strains,

$$\begin{cases} \varepsilon_{zz}(n,s,z,t) = \varepsilon_{zz}^0(s,z,t) + n\varepsilon_{zz}^n(s,z,t) \\ \varepsilon_{zz}^0(s,z,t) = w_0'(z,t) + \theta_x'(z,t)y(s) + \theta_y'(z,t)x(s) - \phi''(z,t)F_w(s) \\ \varepsilon_{zz}^n(s,z,t) = \theta_y'(z,t)\dfrac{dy}{ds} - \theta_x'(z,t)\dfrac{dx}{ds} - \phi''(z,t)a(s) \end{cases} \tag{7}$$

shear strain and transverse shear strains,

$$\begin{cases} \gamma_{sz}(s,z,t) = \gamma_{sz}^0(s,z,t) + 2\dfrac{A_C}{\beta}\phi'(z,t) \\ \gamma_{sz}^0(s,z,t) = [u_0'(z,t) + \theta_y(z,t)]\dfrac{dx}{ds} + [v_0'(z,t) + \theta_x(z,t)]\dfrac{dy}{ds} \\ \gamma_{nz}(s,z,t) = [u_0'(z,t) + \theta_y(z,t)]\dfrac{dy}{ds} - [v_0'(z,t) + \theta_x(z,t)]\dfrac{dx}{ds} \end{cases} \tag{8}$$

where $\varepsilon_{zz}^0, \gamma_{sz}^0$ are the normal strain and the shear strain components, respectively on the mid-surface of the "Thin-Walled Box Beam".

The stress resultants "N`$s$" and stress couples "$L$`s" can be reduced to the following expressions:

The <u>stress resultants</u> "N`s":

$$\begin{cases} \begin{Bmatrix} N_{zz} \\ N_{sz} \end{Bmatrix} = \begin{bmatrix} K_{11} & K_{12} & K_{13} & K_{14} \\ K_{21} & K_{22} & K_{23} & K_{24} \end{bmatrix} \begin{Bmatrix} \varepsilon_{zz}^0 \\ \gamma_{sz}^0 \\ \phi' \\ \varepsilon_{zz}^n \end{Bmatrix} \\ N_{nz} = A_{44}\gamma_{nz} \end{cases} \tag{9}$$

The <u>stress resultants moments</u> "L`s",

$$\begin{cases} \begin{Bmatrix} L_{zz} \\ L_{sz} \end{Bmatrix} = \begin{bmatrix} K_{41} & K_{42} & K_{43} & K_{44} \\ K_{51} & K_{52} & K_{53} & K_{54} \end{bmatrix} \begin{Bmatrix} \varepsilon_{zz}^0 \\ \gamma_{sz}^0 \\ \phi' \\ \varepsilon_{zz}^n \end{Bmatrix} \end{cases} \tag{10}$$

In the above expressions.(9) and (10) the reduced stiffness coefficients $\left(K_{ij}\right)$ are defined in [14,15].

The kinetic energy, the strain energy and the work of external forces are calculated using the previous strain-displacement relationships, sectional effective stiffness matrix, and external forces. By substituting those values into the "Hamilton's Principle", the "Governing System of Equations" can be obtained. The "Rotating Thin-Walled Composite Box Beam Theory" produces a linear relationship between the section structural loads and the strain measures [15-17]. Then,
"Hamilton`s Principle" and "Variational Formulation",

$$\left| \begin{array}{l} \int_{t_1}^{t_2} (\delta T - \delta V + \delta W) dt = 0 \\ at \quad t = t_1, t_2 \qquad \delta u_0 = \delta v_0 = \delta w_0 = \delta \theta_x = \delta \theta_y = \delta \phi = 0 \end{array} \right. \tag{11}$$

the kinetic energy of the system is,

$$\delta T = \iiint \rho \dot{R} \delta \dot{R} \quad dndsdz \tag{12}$$

and the potential energy of the system is,

$$\left| \begin{array}{l} \delta V = \iiint \sigma_{ij} \delta \varepsilon_{ij} \quad dndsdz \\ = \delta \left\{ \frac{1}{2} \int_0^L \oint_C \sum_{k=1}^{N} \int_{h(k)} [\sigma_{zz} \varepsilon_{zz} + \sigma_{sz} \varepsilon_{sz} + \sigma_{nz} \varepsilon_{nx}]_{(k)} dndsdz \right\} \end{array} \right. \tag{13}$$

and, the work of the external forces,

$$\delta W = \int_0^L (p_y(z,t) \delta v_0(z,t) + (m_z + b_w^{'}) \delta \phi(z,t)) dz \tag{14}$$

Taking into account the present structural configuration and model, the entire state of stress or rather the "System" splits exactly into (i) flap / twist / vertical transverse shear $\left(v_0, \phi, \theta_x\right)$, respectively and (ii) extension / lateral bending / lateral transverse shear $\left(u_0, w_0, \theta_y\right)$, respectively.

The next step in the theoretical formulation is to consider the "Aerodynamic Model" as is done in the following section.

"Incompressible Unsteady Flow" as "Aerodynamic Model"

In general, there are three approaches as well as viewpoints in aerodynamic modeling of aeroelasticity problems. These viewpoints include such concepts as steady flow, semi-steady flow and unsteady flow in different flight regimes. The steady and quasy-steady flows contain errors in predicting the "flutter boundary". Consequently, it is better and more accurate to use the unsteady flows to calculate the realistic aeroelastic behavior and response. The "Aerodynamic Strip Method" based on "Wagner Function" in "Unsteady Incompressible Flow" has been used to simulate incompressible unsteady aerodynamic effects in the "State Space" form. The "Wagner Function" based aerodynamic models provide an efficient, general, and convenient approach to describe the incompressible unsteady flows. In fact, for the incompressible unsteady flows the formulation based on "Wagner Function" is much simpler than other formulations (such as the "Doublet Lattice Method"). Aforementioned method is much suitable for the "aeroelastic response" and "flutter analysis". The "Unsteady Aerodynamic Lift and Pitching Moment (L_{ae} and T_{ae})" about the reference axes, based on the "Strip Theory" in "Aerodynamics of Incompressible Unsteady Flow" are expressed as in [18,19],

$$\left| \begin{array}{l} L_{ae}(z,t) = -\pi \rho_\infty b^2 [\dot{w}_{0.5c}(z,t)] - \\ 2\pi \rho_\infty b \times \left\{ \begin{array}{l} w_{0.75c}(z,t)(\phi_w)(\frac{U_n t}{b}) + \\ \int_0^t \frac{dw_{0.75c}(t_0)}{dt_0} (\phi_w)(\frac{U_n}{b}(t - t_0)) dt_0 + \end{array} \right\} \end{array} \right. \tag{15}$$

$$\left| \begin{array}{l} T_{ae}(z,t) = -\pi \rho_\infty b^3 [\frac{1}{2} U_n \dot{\phi} - U_n a \dot{\phi} + a \ddot{v}_0 + b(\frac{1}{8} + a^2) \ddot{\phi}] - \\ 2\pi \rho_\infty U_n b^2 (\frac{1}{2} + a) \times \left\{ \begin{array}{l} w_{0.75c}(z,t)(\phi_w)(\frac{U_n t}{b}) + \\ \int_0^t \frac{dw_{0.75c}(t_0)}{dt_0} (\phi_w)(\frac{U_n}{b}(t - t_0)) dt_0 + \end{array} \right\} \end{array} \right. \tag{16}$$

where "U_n" is the free stream velocity normal to the leading edge of the blade, $v_0\left(z,t\right)$ denotes the plunging displacement of the points on the reference axis and $\phi\left(z,t\right)$ defines the pitching about this axis at each point. Also "$w_{0.5c}$" and "$w_{0.75c}$" are the downwash at the mid-chord and three quarter chord of the blade and "ϕ_w" is "Wagner's Function". In order to express L_{ae} and T_{ae} in the "state space" form, the quasi-polynomial approximation of Wagner's function is used,
"Wagner Function $\left(\phi_w\right)$" is approximately given by [20]:

$$(\phi_w)(\tau) = 1 - c_1 e^{-\varepsilon_1 \tau} - c_2 e^{-\varepsilon_2 \tau} \tag{17}$$

and the constants are,

$c_1 = 0.165, \quad c_2 = 0.335, \quad \varepsilon_1 = 0.0455, \quad \varepsilon_2 = 0.3$

In the other word,

$$(\phi_w)(\tau) = \left[1 - \sum_{i=1}^{n} \alpha_i \exp(-\beta_i \tau)\right] H(\tau) \tag{18}$$

where, the two aerodynamic lag terms are used for each "Wagner Function". For instance, $n=2$ and as a result, there are, totally, 2 aerodynamic lag terms in the description of the 2-D unsteady aerodynamic loads in the incompressible flow. Also, in the above Eq.(18), "$H(\tau)$" is the definition of the unite step function. Also, in above equations, "$\tau = \frac{U_n t}{b}$" is a dimensionless quantity. Using the notation of Ref. [15,16] and denoting the following expressions,

$$\int_0^t \frac{dw_{0.75c}(t_0)}{dt_0}(\phi_w)(\frac{U_n}{b}(t-t_0))dt_0 = D(z,t) \tag{19}$$

where D`s are given as,

$$D_1(z,t) = w_{0.75c}(z,t) - \sum_{i=1}^{n} \alpha_i B_i(z,t) \tag{20}$$

Finally, based on these equations, the explicit expressions of "Unsteady Aerodynamic Lift $L_{ae}\left(z,t\right)$" and the "Unsteady Aerodynamic Pitching Moment $T_{ae}\left(z,t\right)$" are given below in Eq.(21) and Eq.(22), respectively. Thus,

$$\begin{vmatrix} L_{ae}(z,t) = -\pi\rho_\infty U_n b^2[\dot{v}_0 - U_n\dot{\phi} + ba\ddot{\phi}] \\ -C_{L\phi}\rho_\infty U_n b[(\dot{v}_0 - U_n\phi_n + ba\dot{\phi} - \frac{b}{2}(\frac{cl}{\pi}-1)\dot{\phi}) \\ -\sum_{i=1}^{n}\alpha_i B_i(z,t)] \end{vmatrix} \tag{21}$$

$$\begin{vmatrix} T_{ae}(z,t) = -\pi\rho_\infty b^3[\frac{1}{2}(\frac{cl}{\pi}-1)U_n\dot{\phi} - U_n a\dot{\phi} + \\ a\dot{v}_0 + b(\frac{1}{8}+a^2)\ddot{\phi}] - (\frac{1}{2}+a)C_{L\phi}\rho_\infty U_n b^2[\dot{v}_0 - U_n\phi - \\ ba\dot{\phi} - \frac{b}{2}(\frac{cl}{\pi}-1)\dot{\phi} - \sum_{i=1}^{n}\alpha_i B_i(z,t)] \end{vmatrix} \tag{22}$$

In the above equations, the quantities $B`s$ have been defined such that, they should satisfy the following set of expressions in the following Eq.(23),

$$\dot{B}_i + (\beta_i \frac{U_n}{b})B_i = \dot{w}_{0.75c}(z,t) \tag{23}$$

GOVERNING SYSTEM EQUATIONS OF PRESENT AEROELASTIC SYSTEM

In the present study, an anisotropic, "Rotating Thin-Walled Composite Box Beam" is employed in order to consider the effects of the fiber orientation and the lay-up configuration on the "aeroelastic stability" and the dynamic response of a helicopter rotor blade in incompressible flow. The kinetic energy, the strain energy, and the work by external forces of the helicopter rotor blade structure, are calculated using strain – displacement relations, the sectional effective stiffness matrix and the external loads or forces. Thus, by simple substation of aforementioned quantities into the "Hamilton`s Principle" and making use of variational principles the two sets of the "Governing System of Equations" of the problem under study are obtained. Furthermore, the assumption of small deformations and small strains theory results in a linear relationship between cross-section external loads and the strain measures. The present "Circumferentially Asymmetric Stiffness (CAS)" [16-17] analytical model takes into account various non – classical effects such as the fiber orientation (or the material anisotropy), the transverse shear strains, the warping inhibition of the cross – section, etc. The present "Rotating Thin – Walled Composite Box Beam", by means of the "Hamilton`s Principle" and the variational calculus yield the two "sets" of the "Governing System of Equations". The first "set" is elastically coupled by the "flap / twist / vertical transverse shear" or $\left(v_0, \phi, \theta_x\right)$ and the second "set" is elastically coupled by the "extension / lateral bending / lateral transverse shear" or $\left(u_0, w_0, \theta_y\right)$. In this study, the second "set", as usual, is not taken into account. The equations of motion corresponding to the first "set" are of interest for the present problem. Then,

$$\begin{vmatrix} \delta v_0 = 0: a_{55}(v_0'' + \theta_x') + a_{56}\phi''' + (T_z v_0')' + L_{ae} = b_1\ddot{v}_0 \\ \delta\theta_x = 0: a_{33}\theta_x'' + a_{37}\phi'' - a_{55}(v_0' + \theta_x) - a_{56}\phi'' = \\ \qquad (b_4 + b_{14})(\ddot{\theta}_x - \Omega^2\theta_x) \\ \delta\phi = 0: a_{65}(v_0''' + \theta_x'') - a_{66}\phi'''' + a_{73}\theta_x'' + a_{77}\phi'' + (T_r\phi')' \\ \qquad + (b_4 - b_5)\Omega^2\phi + T_{ae} = (b_4 + b_5)\ddot{\phi} - \\ \qquad (b_{10} + b_{18})(\ddot{\phi}'' - \Omega^2\phi'') \end{vmatrix} \tag{24}$$

where the "Unsteady Aerodynamic Lift $L_{ae}\left(z,t\right)$" and the "Unsteady Aerodynamic Pitching Moment $T_{ae}\left(z,t\right)$" are expressed in Eqs.(21) and (22) respectively. Centrifugal forces appear in the flap and twist equations With "T_z" and "T_r" as centrifugal stiffening expressions, respectively. "T_r" plays the role of torsional stiffness induced by the centrifugal force field. Also, the corresponding "Boundary Conditions" at $z=0$ from Eq.(25) are,

$$v_0 = \theta_x = \phi = 0 \quad also \quad d\phi/dz = \phi' = 0 \tag{25}$$

and $z = L$ yields the following:

$$\begin{vmatrix} \delta v_0 = 0 : a_{55}(v_0' + \theta_x') - a_{56}\phi''' + b_1\Omega^2 R(z) = 0 \\ \delta\theta_x = 0 : a_{33}\theta_x' + a_{37}\phi' = 0 \\ \delta\phi = 0 : a_{65}(v_0'' + \theta_x') - a_{66}\phi''' + a_{73}\theta_x' + a_{77}\phi' + \\ \qquad (b_{10} + b_{18})\ddot{\phi}'' + b_1\Omega^2 R(z) I_p \phi' = 0 \\ \delta\phi' = 0 : a_{56}(v_0' + \theta_x) - a_{66}\phi'' = 0 \end{vmatrix} \tag{26}$$

where T_z, T_r and $R(z)$ are given as,

$$\begin{vmatrix} R(z) = R_0(L - z) + \frac{1}{2}(L^2 - z^2), \\ T_z(z,t) = b_1\Omega^2 R(z), \\ I_p = b_4 + b_5, I_{pm} = \dfrac{2I_p}{mb_0 + mt_0}, I_{ph} = \dfrac{I_{pm}}{\beta} \\ T_r(z,t) = T_z I_{ph} \end{vmatrix} \tag{27}$$

and where $\left(a_{ij}\right)$ and $\left(b_i\right)$ and $\left(mb_0, mt_0\right)$ in the above Eqs.(24), (26) and (27) are defined in [15-17].

NUMERICAL SOLUTION PROCEDURE

The "Numerical Method of Solution" employed here is going to be briefly explained. In order to form the mass, stiffness and damping matrices of non-conservative aeroelastic systems, the "Extended Galerkin's Method (EGM)" and the "Method of Separation of Variables" have been used. After that, by transforming matrices into the form of "state space", an eigenvalue analysis has been developed. The real part of the eigenvalues represents the damping and the imaginary parts represent the frequency. Therefore, by solving the resulting coupled linear "Governing System of Dynamic Equations", the "flutter" and "divergence" speeds for various laminate configurations with different geometric and material properties were obtained. Then, by solving the aforementioned dynamic equations in the time domain, the aeroelastic responses of the composite helicopter rotor blade for different flight speed and angular velocity have been computed. The present numerical results were compared with the same existing analytical results.

In order to solve this set of equations in Eq. (24) the "Extended Galerkin`s Method (EGM)" is employed. For this purpose, the aerodynamic and the structural variables have to be discretized through time. Hence, the assumed mode shapes, are as follows,

$$\begin{vmatrix} v_0(z,t) = \psi_v^T(z) q_v(t) & B_1(z,t) = \psi_{B_1}^T(z) q_{B_1}(t) \\ \theta_x(z,t) = \psi_x^T(z) q_x(t) \quad , & B_2(z,t) = \psi_{B_2}^T(z) q_{B_2}(t) \\ \phi(z,t) = \psi_\phi^T(z) q_\phi(t) & B_3(z,t) = \psi_{B_3}^T(z) q_{B_3}(t) \end{vmatrix} \tag{28}$$

in which "ψ_i" are the so-called "admissible functions" which satisfy the "Geometric Boundary Conditions" of the problem. The "State Vector" or the column matrix of time dependent variables for the incompressible flow is defined as in the following,

$$\left\{q\right\} = \left\{ q_v^T \quad q_\phi^T \quad q_x^T \quad q_{B_1}^T \quad q_{B_2}^T \quad q_{B_3}^T \right\}^T \tag{29}$$

After some manipulations, the "aeroelastic general equation" are finally obtained, in terms of the development of the mass, the stiffness and the damping matrices, such that,

$$(M_s + M_{ae})\ddot{q} + (C_{ae})\dot{q} + (K_s + K_{ae})q = \left\{0\right\} \tag{30}$$

Where "M_s" and "M_{ae}" are the structural and aerodynamic mass matrices and "C_{ae}" is the aerodynamic damping matrix and "K_s" and "K_{ae}" are the structural and aerodynamic stiffness matrices, respectively.
If the "state vector" is redefined as,

$$\left\{X\right\} = \left\{ \left\{q\right\}^T \quad \dot{q}_v^T \quad \dot{q}_\phi^T \quad \dot{q}_x^T \right\}^T \tag{31}$$

Then, the "state space" form of the dominant "Governing System of Equations" in Eq. (24) becomes,

$$\begin{bmatrix} C_{ae} & M_{ae} + M_s \\ [I] & [0] \end{bmatrix} \left\{\dot{X}\right\} + \begin{bmatrix} K_{ae} + K_s & [0] \\ [0] & -[I] \end{bmatrix} \left\{X\right\} = \left\{0\right\} \tag{32}$$

where $\left[I\right]$ is the unit matrix and $\left[0\right]$ is the zero matrix.

The above "System" can be rewritten in a more compact "state vector" form, Then, the "Governing System of Equations" is,

$$\begin{vmatrix} \left\{\dot{X}\right\} = \left[A\right]\left\{X\right\}, \\ \left[A\right] = -\begin{bmatrix} C_{ae} & M_{ae} + M_s \\ [I] & [0] \end{bmatrix}^{-1} \begin{bmatrix} K_{ae} + K_s & [0] \\ [0] & -[I] \end{bmatrix} \end{vmatrix} \tag{33}$$

Now, to obtain the specific values related to the Eq.(33), the "Closed Form Solution" is assumed to be,
General solution (closed form),

$$\left\{X\right\} = \left\{X_0\right\} e^{\lambda\tau} \tag{34}$$

where $\left\{X_0\right\}$ is a constant vector and "λ" is a constant scalar, both of them being, in general, the complex

quantities. After inserting Eq.(34) into Eq.(33), the following "Eigenvalue Problem" is obtained,

$$\{A\}\{X_0\} = \lambda\{X_0\} \quad (35)$$

In the above, Eq.(35) yields the eigenvalues and the corresponding eigenvectors (which are complex quantities).

It is also important to note here that the "Governing System of Equations" is finally reduced or rather converted into an "Eigenvalue Problem" in Eq. (35).

In Eq.(35), the real part of a particular eigenvalue indicates the damping value and the imaginary part represents the frequency. Thus, by means of solving the above equations in the time domain, the various aeroelastic responses of the "Rotating Thin – Walled Composite Box Beam" (or rather the present rotor blade model) can be computed.

SOME NUMERICAL RESULTS AND VALIDATION

Validation of Incompressible Aero-Elastic Pattern

In this study, the Ref. [16] is used to evaluate the accuracy of the results of present aero-elastic incompressible flow model. This investigation [16] consists of aeroelastic instability of "Thin Walled Composite Box Beam" in an incompressible flow. The geometric and mechanical properties of the "Thin Walled Composite Box Beam" are considered in Ref. [16]. The present numerical results are compared with the results of the analytical results from Ref. [16]. Hence, the inspection of the results in Table. (1) provides the verification of and the validation of the present model considered in this study.

Table.1 . Comparison of the instability results of the composite box beam $\theta = -20^0, \Omega = 0$

a	Ref [16]		Present work	
	$U_F(m/s)$	$\omega_f(Hz)$	$U_F(m/s)$	$w_f(Hz)$
***a* = 0**	100	3.59	102	3.54
***a* = - 0.2**	127	3.62	128	3.56

Investigation of Aero-Elastic Model Response in Incompressible Flow

In this section, the "aeroelastic model response" in incompressible flow is investigated. The implication of warping restraint and the transverse shear effects on the response are also considered. The geometric and material specifications of the "Rotating Thin-Walled Composite Box Beams" with CAS lay-up are listed in Tables.(2) and (3). Note that, in the actual implementation, the first 5 structural modes and 2 aerodynamic lag terms for "Wagner Function" (see also Eq.(18)) are used, (i.e., m = 5, n=2). This rotor blade is capable of flying in incompressible flow regime.

Figure. (4) illustrate the Flap and the Twist responses for model helicopter rotor composite blade for $\Omega = 300rpm, U_n = 80m/s, \frac{c}{R} = 0.07$.

Table. 2. Rectangular Cross section "Thin-Walled Composite Box Beam" (Geometric Specifications)

Geometric specification	value
Width, $2w$	0.23 m
Depth, $2d$	0.088 m
Wall thickness, h	0.012 m
rotor blade chord, $2b$	0.5 m

Table. 3. Rectangular Cross Section "Thin-Walled Composite Box Beam" (Material properties)

Material specification	value
E_{11}	206.8 (Gpa)
$E_{22} = E_{33}$	5.17 (Gpa)
$G_{12} = G_{13}$	3.1 (Gpa)
G_{23}	2.55 (Gpa)
$\mu_{12} = \mu_{13} = \mu_{23}$	0.25
ρ	1528 (kg/m^3)

Investigation of Rotor Blade Flap Response of "Composite Helicopter Rotate Blade" Model on the Basis of Fiber Orientation (θ) Variation

In examining responses in incompressible flight regimes, we investigated the effect of the fiber lay-up on the rotor blade flap response. Then, Figure. (5). have been sketched for the flap mode for fiber orientation $\theta = -20^0, -40^0, -60^0, -80^0$. The flight forward speed and rotor blade angular velocity of the present model and "a" parameter have been considered for $U_n = 80m/s, \Omega = 300rpm$ and $a = 0$ respectively. The longest time needed for the damping of the responses is seen for $\theta = -80^0$. The angle "θ" changes from $\theta = 0^0$ towards $\theta = -80^0$, the blade flap response amplitude increases and the response damping time increases.

Investigation of Rotor Blade Flap Response of "Composite Helicopter Rotate Blade" Model Based on Distance Variation Between Aero-Dynamic Center and Elastic Center (ab)

In real helicopter rotor blades, there exists a distance between the aerodynamic center and the elastic center

which is marked with "ab" magnitude in Figure.(1). This distance has an important effect on the "aeroelastic steadiness" of the rotor blades. Thus, Figures.(6). illustrate oscillations response for coefficients $a = 0.3, 0, -0.3, -0.6$,respectively. The forward velocity and rotor blade angular velocity of the present model and fiber orientation have been considered for $U_n = 80m/s, \Omega = 300rpm$ and $\theta = -20^0$ respectively.

The more positive coefficient "a" becomes the more "flutter speed" increases, and consequently, the rotor blade can fly in high speed. With regards to Figure.(6) , for the flap mode, the response amplitude for $a = -0.6$ is larger than those of $a = -0.3, 0$ and $a = 0.3$ and the response full damping time also gets larger. In general, with the value "a" becoming more negative, the response amplitude increases. Consequently, the damping time of oscillations becomes longer. This damping time for flap mode is around 1 seconds.

Investigation of Rotor Blade Flap Response of "Composite Helicopter Rotate Blade" Model Based on Forward speed (U_n) Variations

Figures.(7). illustrate the effects of different forward speed on rotor blade flap responses. The flap responses for the forward speeds $U_n = 40m/s, 60m/s, 80m/s$ are considered in Figure.(7). The fiber orientation and rotor blade angular velocity of the present model and "a" parameter have been considered for $\theta = -60^0, \Omega = 300rpm$ and $a = 0$ respectively.

As the forward velocity increases, the tip rotor blade flap response amplitude decreases. Likewise, the time needed for response damping also decreases in a way that this time for $U_n = 80m/s$ is around $t = 1\sec$. As for $U_n = 60m/s$ and $U_n = 40m/s$, this time continues to increase.

Investigation of Rotor Blade Flap Response of "Composite Helicopter Rotate Blade" Model Based on Angular Velocity (Ω) Variations

With regards to Figure.(8), for the flap mode, this Figure illustrate the effects of different angular velocity on rotor blade flap responses in fixed forward velocity. The flap responses for the angular velocity $\Omega = 100rpm, 200rpm, 300rpm$ are considered in Figure.8. The fiber orientation and rotor blade forward velocity of the present model and "a" parameter have been considered for $\theta = -60^0, U_n = 80m/s$ and $a = 0$ respectively.

As the angular velocity increases, the tip rotor blade response amplitude for flap mode decreases. Furthermore, the time needed for response damping also decreases in a way that this time for $\Omega = 300rpm$ is around $t = 1\sec$.

BRIEF CONCLUDING REMARKS

The present study investigates the behavior of a "Rotating Thin-Walled Composite Box Beam" as the helicopter rotor blade model made of composite materials in an incompressible unsteady flow. To this end, computer code has been developed to simulate the aero-elastic behavior of the rotor blade based on Librescu "Rotating Thin-Walled Composite Box Beam" structural model and incompressible aerodynamics based on "Wagner Function". A careful analysis of the numerical results obtained from this software revealed that the flutter frequency is zero for positive angles of fiber orientation and has a certain value for negative angles. This means that "rotor blade unsteadiness" occurs in the form of "divergence" for positive angles and in the form of "flutter" for negative angles. Moreover, investigation of rotor blade behavior for different beam modes showed that as the rotor blade core moves toward the wing tip, the distance between the rotor blade aerodynamic center and the elastic center increases and "ab" value becomes highly positive. This leads to an increase in the "rotor blade steadiness" and the occurrence of the modes response damping in shorter period of time.

REFERENCES

[1] I. H. Marshall and H. Demuts (Editors), 1998, "Supportability of Composite Airframes and Aerostructures", Elsevier Applied Science Punlishers, New York.

[2] D. H. Hodges, R. A. Ormiston, "Stability of Elastic Bending and Torsion of Uniform Cantilever Rotor Blade in Hover with Variable Structural Coupling", NASA TN D-8192, April, 1976.

[3] P. P. Friedmann, "Effect of Modified Aerodynamic Strip Theories on Rotor Blade Aeroelastic Stability", AIAA J 1977; 15(7):932-40.

[4] N. T. Sivaneri, I. Chopra, "Dynamic Stability of a Rotor Blade Using Finite Element Analysis", AIAA J 1982;20(5):716-23.

[5] C. H. Hong, I. Chopra, "Aeroelastic Stability Analysis of a Composite Rotor Blade", J Am Helicopter Soc 1985;30(2):57-67.

[6] O. Rand, "Periodic Response of Thin-Walled Composite Helicopter Blades", J Am Helicopter Soc 1991;36(4):3-11.

[7] L.W. Rehfield, "Design analysis Methodology for Composite Rotor Blades", Proceedings of the Seventh DOD/NASA Conference on Fibrous Composites in Structural Design, AFWAL-TR-85-3094, June 1985, pp. 1–15.

[8] L.W. Rehfield, A.R. Atilgan, D.H. Hodges, "Nonclassical Behavior of Thin-Walled Composite Beams with Closed Cross Sections", Proceedings of the American Helicopter Society National Technical Specialists Meeting: Advanced Rotorcraft Structures,Williamsburg, VA, October 1988, pp.

42–50.
[9] R. Chandra, I. Chopra, "Experimental-Theoretical Investigation of the Vibration Characteristics of Rotating Composite Box Beams", Journal of Aircraft 29 (4) (1992) 657–664.
[10] E. C. Smith, I. Chopra, "Aeroelastic Response and Blade Loads of a Composite Rotor in Forward Flight", In:Proceedings of AIAA/ASME/ASCE/AHS/ACS 33rd Structures, Structural Dynamics and Materials Conference. Dallas, Texas, 1992, P. 1996-2014.
[11] O. Song, L. Librescu, S.Y. Oh, "Vibration of Pretwisted Adaptive Rotating Blades Modeled as Anisotropic Thin-Walled Beams", AIAA Journal 39 (2) (2001) 285–295
[12] L. Librescu, O. Song, 1991, "Behavior of Thin-Walled Beams Made of Advanced Composite Materials and Incorporating Non-Classical Effects" Appl Mech Rev 1991; 44(11): S174-80. Part.2
[13] O. Song, 1990, "Modeling and Response Analysis of Thin-Walled Beam Structure Constructed of Advanced Composite Materials" PhD Thesis, Virginia Polytechnic Institute and State University.
[14] Z. Qin, L. Librescu, 2003, "Dynamic Aeroelastic Response of Aircraft Wing Modeled as Anisotropic Thin-Walled Beams", J Aircraft 2003; 40(3).
[15] Z. Qin, 2001, "Vibration and Aeroelasticity of Advanced Aircraft Wing Modeled as Thin-Walled Beams – Dynamics, Stability and Control", PhD Thesis, Virginia Polytechnic Institute and State University.
[16] H. Haddadpour, M. A. Kouchakzadeh , F. Shadmehri, 2008, "Aeroelastic Instability of Aircraft Composite Wings in an Incompressible Flow" J. of composite structure 83 , pp 93-99.
[17] L. Librescu, O. Song, 2006, "Thin Walled Composite Beam", Springer, Dordrecht, the Netherlands, 2006
[18] EH. Dowell, EF, Crawley, HC Curtiss, DA, Peters, RH, Scanlan, F. Sisto, 1995, "A Modern Course in Aeroelasticity", Kluwer Academic Publisher.
[19] J.G. Leishman, "Unsteady aerodynamics", in: Principles of Helicopter Aerodynamics, Ch. 8, Cambridge University Press, Cambridge, UK, 2000, pp. 302–377.
[20] R.L. Bisplinghoff, H. Ashley, R.L. "Halfman, Aeroelasticity", Dover Publications, New York, 1996.

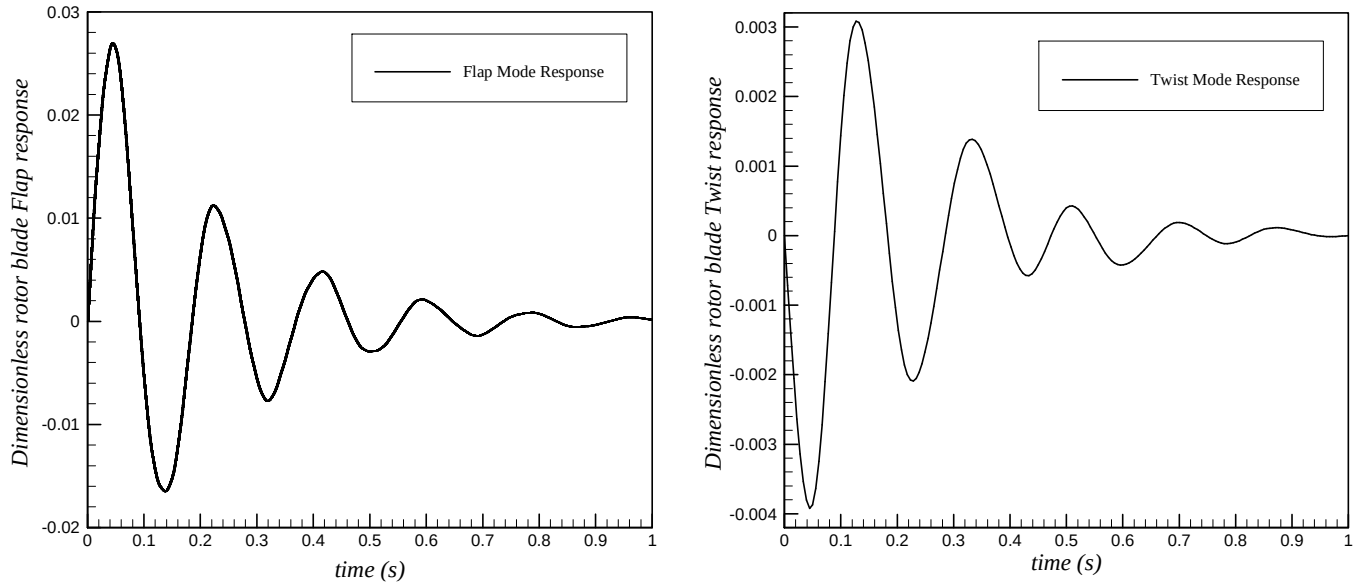

Figure. 4. Rotor blade Flap and Twist response for $\theta = -60^0, \Omega = 300rpm, U_n = 80m/s, a = 0$

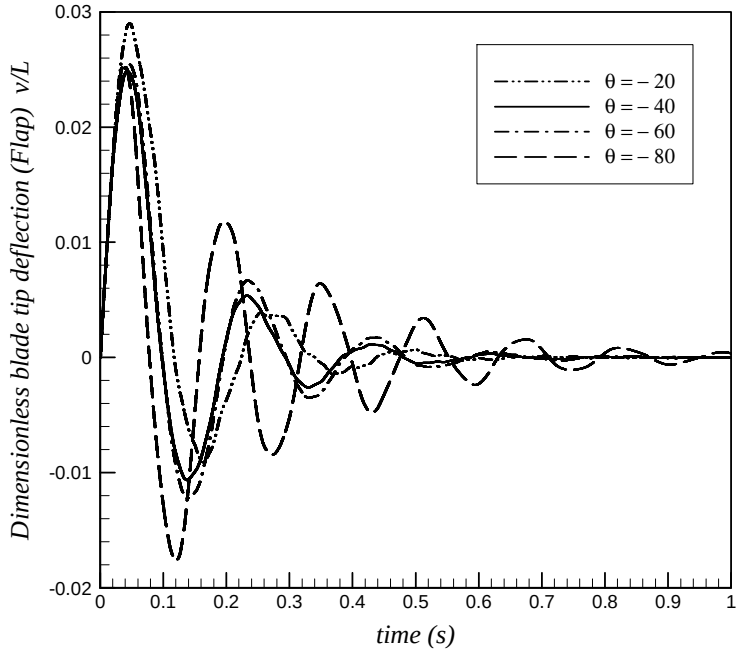

Figure. 5. Rotor blade flap response for the variation of fiber angles for $\theta = -20^0, -40^0, -60^0, -80^0$ and $\Omega = 300rpm, U_n = 80m/s, a = 0$

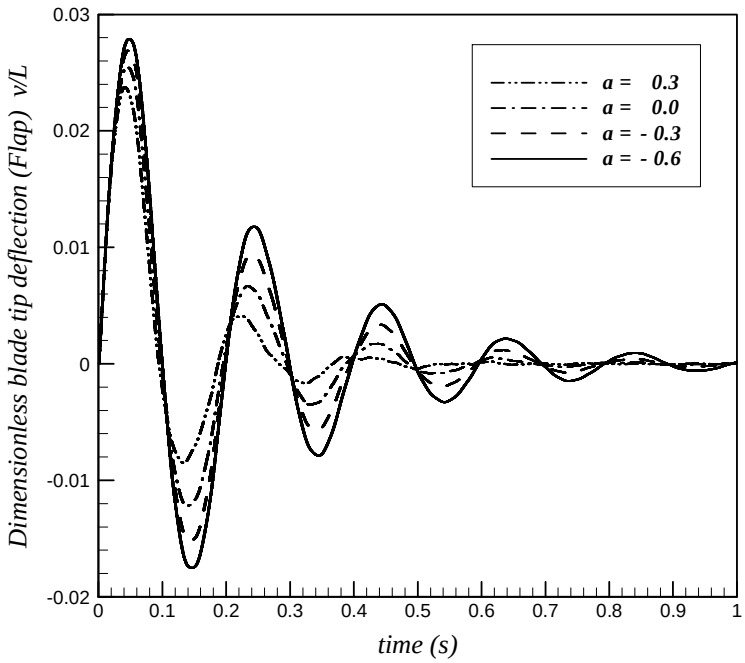

Figure. 6. Rotor blade flap response for the offset between aerodynamic center and the elastic center for $\theta = -20^0, \Omega = 300rpm, U_n = 80m/s$

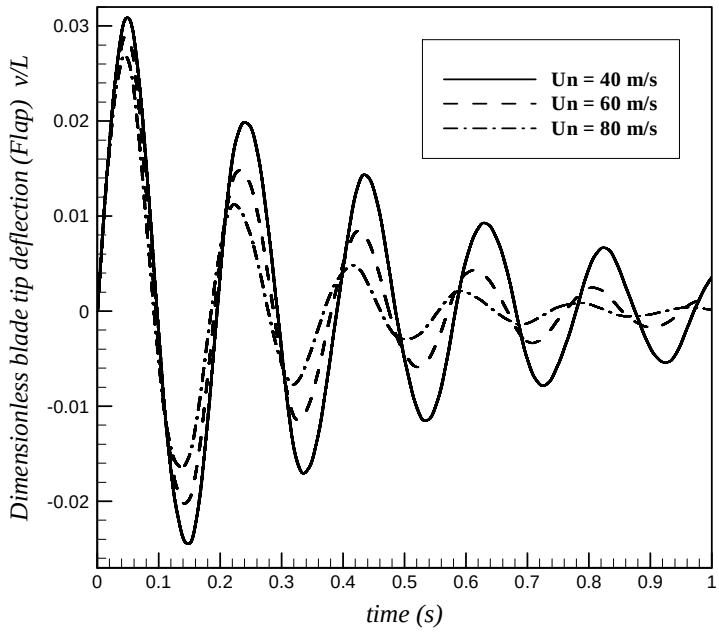

Figure. 7. Rotor blade flap response for different forward flight speed for $\theta = -60^0, \Omega = 300rpm, a = 0$

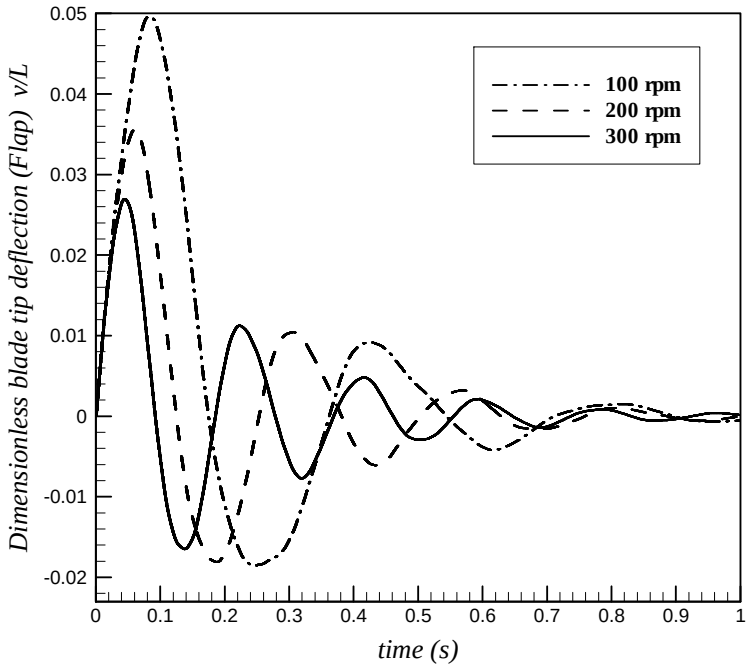

Figure. 8. Rotor blade flap response for different rotor angular velocity for $\Omega = 100rpm, 200rpm, 300rpm$ and $\theta = -60^0, U_n = 80m/s, a = 0$